RADIATIVE AND FREE-CONVECTIVE HEAT TRANSFER FROM A FINITE HORIZONTAL PLATE INSIDE AN ENCLOSURE*

Peter Hrycak and D. J. Sandman

New Jersey Institute of Technology
Newark, New Jersey 07102

ABSTRACT

An experimental and analytical investigation of heat transfer from a horizontal, thin, square plate inside of an enclosure has been carried out. Experimental results have been obtained from both the upward-facing and the downward-facing sides of the heated plate. Starting with the integrated momentum and energy equations, approximate solutions have been obtained for heat transfer in the laminar and the turbulent regime that correlate well with own experimental data and the results of other investigators. Radiative heat transfer correction was given a special attention. Effects of the enclosure-related recirculation of the test fluid, as well as effects of simultaneous heat transfer on both sides of the plate, caused an early transition, and indicated a high level of internal turbulence.

INTRODUCTION

Heat transfer from horizontal, heated plates by far has not received the attention accorded to other geometries. There appears still to exist a general scarcity of representative experimental data, in particular in the turbulent regime. As heat transfer by free convection, for moderate temperature differentials, is of the same order of magnitude as that by radiation, the need for radiation correction during experimentation cannot be disregarded. Therefore, the experimental results below have been carefully checked for the effects of radiation. Also, equations of the boundary-layer type are set up, describing free convection on both sides of a horizontal plate of finite dimensions, heated electrically. Similarity is assumed for both the velocity and temperature profiles. These assumptions are then justified by a close agreement between the results of the analysis and the experimental findings and the literature on the subject. The solutions obtained apply for laminar as well as for turbulent free convection. Due to highly sheltered conditions inside the chamber where the present experiments were carried out, undesirable disturbances like uncontrollable small air movements were eliminated. Ample space between the walls of the chamber and the test plate should have made the resulting free convective flow essentially undisturbed by the presence of the confining walls.

SYMBOLS

A_1 area of specimen, m^2

a thermal diffusivity, m^2/s

$\underline{a}$ constant in reference velocity equations, s^{-1}

* This work has been partially supported under NSF Grant No. MEA- 81-19471

c_p	specific heat at constant pressure, J/(K kg)
Gr_L, Gr^*	Grashof number, $g\beta L^3(T_w - T_\infty)/\nu^2$, Gr_L/L^3, m^{-3}
h	heat transfer coefficient, $W/(m^2K)$
k, $\underline{k}$	thermal conductivity, W/(m K); empirical constant in expression for $\underline{a}$
K	numerical constant in expressions for the Rayleigh number
P	pressure, N/m^2
Pr	Prandtl number, ν/a
q, Q	heat flux density, W/m^2; heat flow rate, W
r, R	coordinate, radial direction, m; radius of test plate, m
$\underline{R}$	gas constant, J/(kg K)
Re_r	Reynolds number, Ur/ν
Ra	Rayleigh number, Gr Pr
T	thermodynamic temperature, K
u, U	dr/dt, velocity ; reference velocity, r-direction, m/s
v	specific volume, m^3/kg
w, W	dz/dt, velocity ; reference velocity, z-direction (perp. to plate), m/s
z	coordinate perpendicular to plate, m
Nu_L	Nusselt number, hL/k
β	cubic expansion coefficient, K^{-1}
δ	boundary-layer thickness, m
ϵ_1	emissivity of specimen
ν	kinematic viscosity, m^2/s
ρ	mass density, kg/m^3
σ	Stefan-Boltzmann constant, $W/(K^4\ m^2)$
θ	reduced temperature, $T - T_\infty$, K

In turbulent regime, u, U, w, and W represent mean-flow velocities

Subscripts:

m condition where maximum velocity occurs in the polynomial expression

w " at the wall of plate

∞ " far away from wall

EXPERIMENTAL TEST SET-UP

In order to make the intended free-convective experiments reasonably accurate, it was decided to test the specimens, that were to be used as the horizontal plates in the tests, independently for emissivity under high-vacuum conditions. Therefore, a high-vacuum chamber was built first, that could contain pressures as low as 10^{-4} mm Hg, with the mean free path of molecules inside long enough to eliminate convection, and to leave only radiation as the mode of heat transfer. Conduction along the specimen support wire, and the heater and the thermocouple wires was calculated to be less than 1% of the total heater input. For free-convective measurements, atmospheric pressure inside of chamber was reestablished.

As the total area of specimens, A_1, represented only 2.1% of the wall area of the vacuum chamber (Fig.1), the required emissivity could be calculated from the formula

$$Q = \epsilon_1 \sigma A_1 (T_1^4 - T_2^4) \tag{1}$$

The emissivities measured with this set-up are seen in Fig.2. They all appear to be of the right order of magnitude, when compared with results from the literature, and appear to be adequate for making radiative-loss corrections in free-convective measurements more realistic.

BASIC EQUATIONS OF THE PROBLEM

Let's now consider natural convection flow of a Newtonian, single species fluid over a horizontal surface in an axisymmetric flow, with the coordinates r and z. The flow is in the steady state, the velocity field consists of $u = dr/dt$ and $w = dz/dt$, and the corresponding temperature field is $T = T(r,z)$. The acting surface force is the pressure, and the body force is the gravitational force, g, all acting on a horizontal plate 86.0 mm in diameter which, in turn, gives rise to convective flow considered positive in the direction towards the center of plate; at edge of plate, $r = 0$. We assume that this flow is amenable to analytical treatment using the boundary-layer theory approach, together with Boussinesq approximation towards the treatment of the variable physical properties. Also, there is assumed similarity of velocity and temperature profiles. Then the continuity, momentum, and the energy equations assume the form

$$\frac{\partial(ru)}{\partial r} + \frac{\partial(rw)}{\partial z} = 0 \tag{2}$$

$$u\frac{\partial u}{\partial r} + w\frac{\partial u}{\partial z} = -\frac{1}{\rho}\frac{\partial P}{\partial r} + \nu\frac{\partial^2 u}{\partial z^2} \tag{3}$$

$$0 = -\frac{1}{\rho}\frac{\partial P}{\partial z} + g\beta(T - T_\infty) \tag{4}$$

$$u\frac{\partial T}{\partial r} + w\frac{\partial T}{\partial z} = a\frac{\partial^2 T}{\partial z^2} \tag{5}$$

with the boundary conditions:

at $z = 0$, $u = w = 0$; $T = T_w = \text{const}$; at the edge of plate, $r = 0$, and $u = 0$ (6)

at $z = \delta$, $u = 0$, $T = T_\infty$; $\partial u/\partial z = \partial T/\partial z = 0$ (7)

On differentiating eq. (4) with respect to r, and integrating it with respect to z, we have

$$-\frac{1}{\rho}\frac{\partial P}{\partial r} = g\beta \int_z^\delta \frac{\partial}{\partial r}(T - T_\infty)\, dz \tag{8}$$

This approach to free convection on a horizontal plate, apparently first outlined by Stewartson [1], for two-dimensional flow, is applied here to three-dimensional, axisymmetric flow. Thus, from the continuity equation, we have

$$w = -\int_o^z \left(\frac{\partial u}{\partial r} + \frac{u}{r}\right) dz \tag{9}$$

Equations (8) and (9), on substitution in eq. (3), after partial integration, yield

$$\frac{1}{r}\frac{d}{dr}\left(r \int_o^\delta u^2\, dz\right) = g\beta \int_o^\delta \left[\int_z^\delta \frac{\partial}{\partial r}(T - T_\infty) dz\right] dz - \nu \left(\frac{\partial u}{\partial z}\right)_w \tag{10}$$

Equation (5) may be transformed in a similar fashion after a partial integration. Letting $\theta = T - T_\infty$, and assuming that δ (hydrodynamic) $\approx \delta$ (thermal), there results

$$c_p \rho \frac{1}{r}\frac{d}{dr}\left(r \int_o^\delta u\theta\, dz\right) = -k \left(\frac{\partial \theta}{\partial z}\right)_w \tag{11}$$

Additionally, letting the velocity and temperature profiles be

$$u = U\,(z/\delta)(1 - z/\delta)^2; \quad \theta = \theta_w (1 - z/\delta)^2 \tag{12}$$

as proposed, for example, by Eckert and Drake for a related problem [2], and letting

$$U = C_1\, r^m \quad ; \quad \delta = C_2\, r^n \tag{13}$$

a speedy solution of eqs. (10) and (11) is obtained. With $\beta = 1/T_\infty$, we get

$$\frac{1}{r}\frac{d}{dr}\left(rU^2\delta\right) = 17.5\, g\beta\, \theta\delta\, d\delta/dr - 105\, \nu(U/\delta), \quad \text{and} \tag{14}$$

$$\frac{1}{r}\frac{d}{dr}\left(rU\theta_w\delta\right) = 60\, a\theta_w/\delta \tag{15}$$

which, after eq. (13) has been substituted, yield

$$(2m + n + 1)C_1^2 C_2\, r^{2m+n-1} = 17.5\, g\beta\, \theta_w n\, C_2^2\, r^{2n-1} - 105\, (C_1/C_2)\, r^{m-n}\nu \quad \text{and} \tag{16}$$

$$(m + n + 1)\, C_1 C_2\, r^{m+n-1} = 60\, a\, r^{-n}/C_2 \tag{17}$$

For similarity solutions, both sides of these equations must be independent of r; this is true if $m = 1/5$ and $n = 2/5$ for the present geometry. Then eqs. (16) and (17) yield, with $Gr^* = Gr/L^3$

$$C_1 = 2.978\, a\, Pr^{4/5}(9/14 + Pr)^{-2/5}\, (Gr^*)^{2/5} \quad \text{and}$$

$$C_2 = 3.548\, Pr^{-2/5}(9/14 + Pr)^{1/5}\, (Gr^*)^{-1/5}$$

from which, together with eq. (13) is calculated the local heat transfer coefficient

$$h_r = q_w/\theta_w \tag{18}$$

while the average heat transfer coefficient becomes

$$h_R = 0.705\ k\ Pr^{2/5}(0.643 + Pr)^{-1/5}(Gr^*)^{1/5}R^{-2/5} \tag{19}$$

In order to obtain a formula for the average heat transfer coefficient based on the side L of an equivalent square plate, we let $L^2 = \pi R^2$, such that L (equivalent) = $\pi^{\frac{1}{2}}R$, $h_R = \pi^{-1/5}$, and $Nu_L = h_L L/k$, or

$$Nu_L = 0.886\ Pr^{2/5}\ (0.643 + Pr)^{-1/5}\ Gr_L^{1/5} \tag{20}$$

For air (Pr = 0.72), this generates the Rayleigh number, $Ra_L = Gr_L Pr$, based on L, or

$$Nu_L = 0.780\ Ra_L^{1/5} \tag{21}$$

for a horizontal square plate heated on the top side only. With the present choice of coordinates, $\delta = 0$ at the edge of plate. In the case of a horizontal plate, heated at both sides, $\delta \neq 0$ at the edges. According to the literature on this subject (cf. reference 3, for example), a horizontal plate heated on both sides has its heat transfer on the upper side appreciably increased by formation of a warm air "bubble" on its lower side. It appears in the present case that increasing the area of plate by about one fifth generates an "effective area" that shows realistically the effect of heating of the bottom side of plate on heat transfer on the upper side in the form of an "effective radius", R_{eff}

$$R_{eff} = 1.095\ R_{actual} \tag{22}$$

to be used as the upper limit in the evaluation of the average heat transfer coefficient

$$h_{R,eff} = 0.816\ k\ Pr^{2/5}\ (0.643 + Pr)^{-1/5}\ Gr^{1/5}/R \tag{23}$$

which, for example, for Pr = 0.72, results in

$$Nu_L = 0.902\ Ra_L^{1/5} \tag{24}$$

The velocity and temperature profiles applicable here as per eqs.(6) and (7) satisfy the physical conditions of the problem at hand, eqs.(2) - (5), and reduce to zero for $z > \delta$. They are also for $z < \delta$ qualitatively what can be reasonably expected in free convective flow under conditions of conservation of mass and energy, regardless of orientation of flow, with exception of a small area near the plate's center, where an upward-pointing jet is generated, as has been already observed by Stewartson [1]. This effect will be accounted for below in a separate discussion. Other velocity and temperature profiles have been considered. It may be seen from the comparison with the experimental results (cf. discussion below) that eqs. (21) and (24) come already reasonably close to physical reality. This is perhaps the best justification of the methods used above, and for the particular u and θ used.

Experience teaches us that in free convection inside an enclosure (cf. McAdams [5], p. 182) turbulence may develop already at relatively low Grashof numbers. For the case of heated, horizontal plates, this is explainable by the destabilizing ef-

fect of the upward-directed buoyant force on the boundary-like layer formed by the fluid flowing in the direction tangential to the plate. For developed turbulent flow, the last term in eq. (10) may be replaced by the semi-empirical expression

$$0.0228\ U^2\ (\nu/U\delta)^p(\delta/\delta_m)^p\ J^{2-p} \tag{25}$$

and the right-hand side of eq. (11) may be defined as

$$0.0228\ c_p\rho\ U\theta_w\ (\nu/U\delta)^p\ Pr^{-2/3}(\delta/\delta_m)^p\ J^{1-p} \tag{26}$$

while the velocity and temperature distribution may be written (cf. Eckert and Jackson [4], and reference 2, p. 324) as

$$u = UJ\ (z/\delta)^{1/q}(1 - z/\delta)^s \quad ; \quad \theta = \theta_w[1 - (z/\delta)^{1/t}] \tag{27}$$

with the exponents q, s, and t determined later.

Since eqs. (25) and (26) were originally based on the maximum velocity in the boundary layer, occurring here at $z = \delta_m$, a normalizing scale factor is introduced in eq. (27), assuring that $u/U = 1.0$ when $z = \delta_m$ applies. It may be shown that u peaks out when $z = \delta_m = \delta/(q \cdot s + 1)$, while the nominal length δ itself signifies to what extent the effect of heating from the plate penetrated the fluid above. The numerical constant in eq. (25) may be approximated by the formula

$$C(p,q) = 1.013\ (0.92\ q + 2.30)^{-pq} \tag{28}$$

based on results of Wieghardt (cf. Schlichting [6], p. 601). With $p = \frac{1}{4}$, eq. (25) becomes the Blasius formula, linked to $q = 7$ in eqs. (27) and (28); when $p = 1/5$, $q = 9$ applies. It is felt that with these changes, eqs. (25) to (28) will be representative of turbulent flow in general, regardless of orientation. Furthermore, eqs. (27) and (28) satisfy the boundary conditions for u and θ at $z = 0$ and $z = \delta$ in a satisfactory manner; with these substitutions, with the required integrations carried out, eqs. (10) and (11) yield the relations

$$J^2\ I_1(1/r)\frac{d}{dr}(rU^2\delta) = I_2\ g\beta\ \theta_w\delta d\delta/dr - K_3U^2(\nu/U\delta)^pJ^{2-p} \quad \text{and} \tag{29}$$

$$J\ I_3(1/r)\ \frac{d}{dr}(rU\delta)\ = K_5\ U(\nu/U\delta)^p\ Pr^{-2/3}\ J^{1-p} \tag{30}$$

Assuming again validity of eq. (13), eqs. (29) and (30) yield after a few transformations the expression for the local Nusselt number, for $m = 1/(2+3p)$, and $n = 2m$,

$$Nu_r = JK_5\ (K_2/K_1)^m(K_5/K_4)^{m(1-3p)}Pr^{-m(1-3p)}(1 + Pr^{2/3}K_4/K_1)^{-m}Ra_r^{\ m} \tag{31}$$

and the average Nusselt number for an equivalent square plate with side L,

$$Nu_L = JK_5(K_2/K_1)^m(K_5/K_4)^{m(1-3p)}Pr^{-m(1-3p)}(1 + Pr^{2/3}K_4/K_1)^{-m}\ \frac{2}{1+3m}^{-\frac{1}{2}m(1-3p)}Ra_L^{\ m} \tag{31a}$$

In eqs. (31) and (31a), the use of J should be considered entirely empirical; the constants K_n below stand for the integrals based on eqs. (27) and (28):

$$K_3 = K_5 = C(p,q)\ (\delta/\delta_m)^p$$

$$K_1 = (2m + n + 1)/(U^2\delta)\int_0^\delta u^2\ dz = (2m + n + 1)\ I_1$$

$$K_2 = n/(\theta_w \delta d\delta/dr) \cdot \int_o^\delta (\int_z^\delta \frac{\partial}{\partial r}\theta \, dz) \, dz = n \, I_2 = n/(2t + 1)$$

$$K_4 = (m + n + 1)/(U\theta_w) \cdot \int_o^\delta u\theta \, dz = (m + n + 1) \, I_3$$

With the use of the Blasius formula for wall shear stress and heat transfer, and s = 8 and t = 4 in eq. (27) results have been obtained that for $5x10^5 < Ra < 10^6$ deviate for less than ± 1.5% from the least-squares fit curve representing the present experimental data, or with m = 4/11 ≈ 0.364, and Pr = 0.72,

$$Nu_L = 0.104 \, Ra_L^{0.364} \tag{32}$$

Here, m = 0.364 is somewhat lower than the experimental value of m = 0.384. The experimental value of m was closely approximated with m = 0.385, when p = 1/5, q = 9, s = 8 and t = 1 in eqs. (27) and (28) was used, but the constant in eq. (31a) was 6% too low vis-à-vis experimental data. In order to get the commonly cited in the literature value of m = 1/3 for the turbulent, free-convective heat transfer from the upward-pointing, horizontal plate by the present method, p = 1/3, q = 5, s = 3, and t = 5 would have been required in eqs. (25) to (28), to yield

$$Nu_L = 0.150 \, Ra_L^{1/3} \tag{32a}$$

Equation (32a) seems to fit experimental data of others, for free convection without recirculation, reasonably well.

The analysis outlined above has been carried out along the lines suggested in references 2 and 4, but modified in several respects to fit the physical requirements of a horizontal plate of finite dimensions, heated and pointing upward. As is stated in reference 4, the exponent of Ra, m = 2/5, fitted very well experimental data for turbulent heat transfer, for free convection on vertical plates and a vertical cylinder. It is seen that semi-empirical approaches can be used to advantage where the exact analysis still fails to give answers of practical significance.

EFFECTS OF FREE CONVECTION ON HEAT TRANSFER AT CENTER OF A HORIZONTAL PLATE

It is obvious from the consideration of the continuity equation alone that free convective flow, for the present geometry, will generate near the center of plate a vertical jet, known as the thermal plume. For purposes of the analysis below, we assume that temperature distribution within the plume is still given by eq. (12), but velocity follows the profile $u = U(z/\delta_m)$, $z \leq \delta_m$, $u = U$, $z > \delta_m$, and

$$U = -\underline{a} \, r \quad ; \quad W = 2^i \underline{a} \, z \quad (r = z = 0 \text{ at center of plate}) \tag{33}$$

where i = 1, axisymmetric flow, and i = 0, plane flow. U and W in eq. (33) satisfy identically the continuity equation. By considering a volume element $(2\pi \, r)^i dr\delta$ and the heat fluxes in and out by convection, as well as by conduction at the bottom through the area element $(2\pi r)^i dr$, after the substitutions for u and θ have been made, there results the expression

$$r^{-i}(\rho c_p \frac{d}{dr} r^i \int_o^\delta u\theta \, dz) = k(\frac{\partial\theta}{\partial z})_w \tag{34}$$

Taking θ from eq. (12) and U as stated above, the integral in eq. (34) may be written, for $\delta_m/\delta \ll 1$, as $I = -ar^2\delta/3$. It yields for δ (which is actually the height of the present thermal plume), the expression

$$\delta = (3a/\underline{a})^{\frac{1}{2}} \tag{35}$$

Using eq. (18), we may write $Nu_r = 2R/\delta$. The still required expression for $\underline{a}$ in eq. (33) is now to be derived. If differential pressure at the center of the plate is proportional to $\underline{k}^4 g\rho\beta\theta_w z/R$, working through a distance dz, that accelerates a fluid element from velocity 0 to W (here $\underline{k}^4$ is the constant of proportionality), one gets $\rho\, \underline{k}^4 \frac{dA}{R} \int_0^z \beta g \theta_w z\, dz = \rho\, dA \int_0^W w\, (dw/dz)\, dz$, on assumption of inviscid flow there, the simple result

$$W = (\beta g \theta_w \underline{k}^4/R)^{\frac{1}{2}}\, z \tag{36}$$

From comparison with eq. (33), eq. (36) yields

$$\underline{a} = (\beta g \theta_w \underline{k}^4/R)^{\frac{1}{2}}/2 = (\underline{k}^4\, Gr\nu^2/R^4)^{\frac{1}{2}}/2, \text{ and} \tag{37}$$

$$Nu_R = (2/3)^{\frac{1}{2}}\, \underline{k}\, Pr^{\frac{1}{2}}\, Gr_R^{\frac{1}{4}} \tag{38}$$

For air with Pr = 0.72, and $L = \pi^{\frac{1}{2}}R$, there results

$$Nu_L = 0.864\, \underline{k}\, Ra_L^{\frac{1}{4}} \tag{39}$$

Integral methods generate useful results that still depend on the approximating polynomials needed to represent u and θ. Thus, if in the present case we use eq. (12) for both u and θ, but with the reasonable constraint that, at $z = \delta_m$, $u = U$, so that eq. (33) is satisfied, we obtain from eqs. (34) and (37)

$$Nu_L = 0.710\, \underline{k}\, Ra_L^{\frac{1}{4}} \tag{39a}$$

Application of the same procedure to the case of an infinite strip (i = 0 in eqs. (33) and (34), u and θ according to eq. (12), and scale factor J = 27/4 applied to u), yields for a strip of the width 2b

$$Nu_b = 0.62\, \underline{k}\, Ra_b^{\frac{1}{4}} \tag{40}$$

It is to be emphasized that eq. (34), obtained from a direct summing up of the convective and conductive contributions to the control volume, differs in sign from eq. (11), obtained from the exact integration of the energy equation, as the chosen coordinate system is different. Also, as the hydrodynamic information on δ is not required, the momentum equation is not at all involved. This greatly simplifies the problem. The use of scale factor J here is needed to satisfy the continuity, eqs. (33).

RELATIONS FOR A HORIZONTAL DOWNWARD-FACING PLATE

It appears that for this geometry the conventional boundary-layer approach is not possible (cf. reference (3), for example). In the present case, the only reason for the movement of fluid is its thermal expansion, due to the contact with the wall at T_w. Therefore, the resulting flow is similar to that occurring in forced, axisymmetric stagnation flow, for which an exact solution of the Navier-Stokes equations exists (reference 6, p. 100). One can expect the fluid temperature near r = 0

to vary, on the average, at some distance below the plate's center, as

$$\theta = (\theta_w/2)\,(1 - r^2/R^2) \tag{41}$$

while simultaneously the velocity terms for the potential flow related to the present problem follow the relations satisfying identically the continuity equation:

$$U = \underline{a}r \quad ; \quad W = -2^{i}\underline{a}z \tag{42}$$

that applies to any incompressible flow, to any geometry. If the fluid in question is perfect gas, the term $\partial P/\partial r$ in eq. (2) may be now transformed as (with $Pv = \underline{R}T$)

$$-\frac{\partial P}{\partial r} = -\left(\frac{\partial P}{\partial T}\right)_v\left(\frac{\partial T}{\partial r}\right) = \rho\underline{R}\,\theta_w r/R^2, \text{ or } -\frac{\partial P}{\partial r} = \frac{P}{T_\infty}\,\frac{\theta_w r}{R^2}$$

using eq. (41) for $T = \theta + T_\infty$. In quiescent gas, $P = g/v$ times an element of length assumed here to be proportional to R. As $\underline{a}$ is still a free constant, we may assume $\underline{k}^4$ to be that constant of proportionality, without the loss of generality. Then,

$-\frac{\partial P}{\partial r} = \underline{k}^4\,\beta g\theta_w r/(Rv) = \underline{k}^4\,Gr^*\nu^2 r(Rv)^{-1}$; letting $\underline{a}^2 = \underline{k}^4\,Gr^*\nu^2/R$, there results

$$-\frac{\partial P}{\partial r} = \rho\,\underline{a}^2 r \tag{43}$$

With the present definition of $\underline{a}$, the pressure-gradient related term in the momentum equation is linked to the acting temperature differential, θ_w. Writing $u = r f'(z)$, and $w = -2 f(z)$, and using a new variable $\eta = (\underline{a}/\nu)^{\frac{1}{2}}z$, eq. (3) above is readily solved. This solution is considered as good for the complete Navier-Stokes equation (reference 6, p. 100). The corresponding solution of the energy equation is available (cf. references 7 and 8). For Pr near unity, we have

$$Nu_r = 0.763\,Pr^{0.4}\,Re_r^{\frac{1}{2}} \tag{44}$$

This is a boundary-layer type solution, based on a exact solution of the Navier-Stokes equations. As here $Re_r = Ur/\nu$, with $\underline{a}$ from eq. (43), we get $Re_r = \underline{k}^2 \cdot (Gr_r\, r/R)^{1/2}$. With Pr = 0.72, and $L = \pi^{\frac{1}{2}}R$, there results for air

$$Nu_L = 0.630\,\underline{k}\,Ra_L^{\frac{1}{4}} \tag{45}$$

where $\underline{k}$ is an experimental constant with a value $\underline{k} \approx 0.5$, in view of the constant K = 0.27 and m = 1/4 in the original correlation due to Saunders and Fishenden, for example [9]. It must be stressed that the present approach is valid only in the region where eqs. (41) and (42) continue to apply, that is, near the center of a circular plate (i = 1), and near the center of a long strip, where r is the distance away from that center, (i = 0). It is of some interest to note that a solution can also be obtained through a direct integration of eq. (11) here, for the same velocity and temperature distributions as in eq. (12), but using a normalizing factor J = 27/4, such that eq. (42) is satisfied. Then from $\delta = (a/\underline{a})^{1/2} \cdot 2.11$, and Pr = 0.72 we have the formula

$$Nu_L = 1.00\,\underline{k}'\,Ra_L^{\frac{1}{4}} \tag{46}$$

The term $\underline{k}'$ expresses the effect of geometry at hand as well as that of the approximating polynomials used. $\underline{k}' = 0.25$ yields K that comes close to the above Saunders and Fishenden result.

It is seen from the discussion above that methods, based both on the exact solution of the Navier-Stokes equations, and on the integrated energy equation method, lead to results that are experimentally verifiable. The relations for streamline

and temperature distribution, calculated by Miyamoto et al. [10] agree qualitatively with our eqs. (41) and (42) and are also suggested by the scheme shown in Fig. 3. In reference 10 are also reported results of Sugawara and Michiochi [11], where K = 0.264 and m = 1/4, that are based on the boundary-layer approximation.

In addition to our eqs. (45) and (46), and to solutions reported in references 10 and 11, there exist also several approximate analytical solutions for the present geometry with m = 1/5 proposed (cf. references 12 and 13). As an explanation for this one should consider that as the exact solution of the governing momentum equation is only valid near r = 0, and with m = 1/4 applicable for the associated heat transfer problem, the flow starting far away from the stagnation point, at the edge of the plate, would result in a quasi-boundary layer flow for which, at least initially, m = 1/5 would be entirely appropriate. The real flow must be actually nonsimilar for a good portion of $0 < r < R$.

DISCUSSION OF EXPERIMENTAL RESULTS

It is interesting to note that the present experimental results show that transition to turbulent flow has already occured as early as at $Gr = 5 \times 10^5$, in agreement with the discussion by McAdams [5], p.182, as the side effect of the confinement in the relatively small vacuum chamber. Our own experimental results on free convection on an upward-facing, horizontal heated plate are shown in Fig. 4. It is seen from Fig. 4 that, for $Ra < 6 \times 10^5$, the experimental data show a reasonable agreement with eq. (24) here, but the number of experimental points for what is considered laminar free convection on a typical upward-pointing, horizontal plate, heated on both sides, is not sufficient for a definitive finding. For comparison, let's consider the formula proposed by Lewandowski and Kubski [14] for a horizontal plate 100 x 60 mm, heated on one side only,

$$Nu = 0.66\, Ra^{1/5} \tag{47}$$

valid for $10^4 < Ra < 10^7$, with a ± 10% error margin, based on experiments with distilled water, glycerine, and soybean oil. Equation (47) is very close to our eq. (21) above. On the other hand, Yousef et al. [15], using Mach-Zehnder interferometer, and for $10^4 < Ra < 10^7$, in air, obtained

$$Nu = 0.622\, Ra^{1/4} \tag{48}$$

for square plates with L = 100, 200, and 400 mm. A similar exponent of Ra has been also obtained by a number of other investigators, for air and for the same geometry: Fishenden and Saunders [16], Bosworth [17], Al Arabi and El-Riedi [18], for example, with K = 0.54, 0.71, 0.70, respectively, all of them for laminar flow. The experimental constants K come very close to that in our eq. (39a) with $\underline{k} = 1.0$, but the range of Ra is similar. The details are shown in Fig. 5. This discussion applies to the average Nusselt numbers only. It is seen that eqs. (21) (horizontal plate heated on one side only), and (24) (horizontal plate heated on both sides), this paper, fall unquestionably into the range of the experimental results reported in the recent literature, although there are differences in the power of the Rayleigh number: m = 1/5 is recommended in reference 14 and in this paper (depending on the flow situation), and in reference 14, while references 15 to 18 report m = 1/4. Also, in this paper, expressions for m = 1/4 and m = 1/3 have been derived.

For turbulent convection results shown in Fig. 4, the least squares fit equa-

tion is

$$Nu_L = 0.0799\ Ra_L^{0.384} \tag{49}$$

that agrees reasonably well with the calculated formula, eq. (32) here, while in reference 14 the experimental result

$$Nu = 0.173\ Ra^{1/3} \tag{50}$$

is proposed, valid for $10^5 < Ra < 10^8$. This result is typical of other experimental findings shown in Fig.5, where, in addition, references 14 to 21 are included. From the review of the above it is seen that $m = 1/3$ is very common for the situations where turbulent free convection takes place on horizontal plates, heated on one side only. For thin plates, of finite size, heated on both sides in finite enclosures, m increases somewhat, due apparently to flow instabilities generated by heat transfer at the bottom of the plate.

To produce the exponent $m = 1/3$ for turbulent, free convective flow in the present case, $p = 1/3$ would have been necessary in eq. (25). It is interesting to see that most of the experimental results for the upward-pointing, heated plate show a remarkable similarity with the results for the vertical walls; the finding of Eckert and Jackson in reference 4 of $m = 2/5$ is worth noting, as it is derived from a semi-empirical theory, as exemplified here by eqs. (25) and (26), and is also backed up by experimental data. It appears that this similarity in free convective heat transfer, in comparing results for horizontal with those for the vertical geometry, lies in the effect of the thermal jet generated at the point where the boundary flow meets head-on and a thermal plume is formed - something like the reverse of the situation depicted in Fig. 3. This aspect has also been analyzed above separately for laminar flow. It is mentioned also by Bosworth in reference 17.

For a horizontal plate facing downward, the controversy concerning the validity of the exponents $m = 1/5$ vs. $m = 1/4$ can be resolved with the analysis of the flow situation, represented here schematically as Fig. 3. The flow on a downward-facing, heated horizontal plate is visualized. It is seen that near the stagnation point a thin boundary-layer-like region exists. Then, farther away, the "boundary-layer" becomes at first thicker, but that thickness is gradually diminishing, as the edge of plate is approached. In this fashion, two kinds of existing analytical solutions, and the corresponding existing dual experimental correlations could be reconciled, as either of the flow modes may predominate in the given experimental set-up.

Our own experimental data are shown in Fig.6. It is seen from Fig.6 that the flow regime there must have been already turbulent for Ra as low as 6×10^5. There is a considerable scatter of the data, indicating a highly unstable flow. Heat transfer intensity, as represented by the corresponding Nusselt numbers, is roughly 50 % of that existing on the upward-facing side of plate, which is also to be found in the literature (cf. reference 19). The results shown in Fig. 6 may be correlated by either of the two equations below. Equation (51) represents the least squares fit

$$Nu_L = 0.0017\ Ra_L^{0.596} \tag{51}$$

while eq. (52) represents the limiting case of flow corresponding to $p = 0$ in eq. (25), or

$$Nu_L = 0.0064\ Ra_L^{0.5} \tag{52}$$

The relatively large exponents of the Rayleigh number in the present case indicate that some recirculation of the air in the test chamber was actually taking place, as the result of simultaneous heating of the bottom and the top of the test plate, thus representing a kind of synergistic effect. Few other data for the present configuration are available for the turbulent regime, for the sake of comparison, except those in reference 19, correlated by a formula that represents simply one-half of the results obtained with the heated flat plate facing upward, with m = 1/3, within ± 10%, as

$$Nu = 0.06\ Ra^{1/3} \tag{53}$$

Obviously, more data for this configuration are still required, and our objective has been to fill this need at least partially. Additional cases for this geometry are discussed in reference 3. A general comparison of results of various investigators is shown in Fig. 7. It is seen from the discussion above that for laminar free convection, on both sides of the horizontal plate, many investigators still use correlations of the type $Nu = K\ Ra^{\frac{1}{4}}$ while some prefer the supposedly more "theoretical" version of $Nu = K\ Ra^{1/5}$. A plausible explanation was given for this discrepancy. In reference 17, K occurring in eq. (53) is given as 0.08, without details.

It is worth noting that Mangler's transformation changes relations valid for two-dimensional flow over a wedge into expressions valid also in three-dimensional (stagnation) flow, without the change of power of Re, for forced convection. A similar phenomenon, by analogy, may be also expected for free convection, with the Reynolds number replaced by its physical equivalent, the Grashof number to one half power. Moreover, the precise values of K would depend on experimental conditions and refinements observed while taking measurements, on geometry, boundary conditions on edges and the details of how the plates were heated. It should also be kept in mind that the left-hand side of the integrated energy equation is the same for both forced and free convection, regardless of the flow regime. The right-hand side of that equation must be changed to an empirical formula when the flow is turbulent, however.

CONCLUDING REMARKS

For turbulent, free-convective heat transfer, characterized by an exponent m > 0.25, most investigators propose m = 1/3. It is conceivable, however, that for cases of really well-developed, rough, non-isotropic turbulence, that exponent may get as high as 0.384 and perhaps even higher than 0.5, as is indicated by the present experiments, for the significantly unstable flow at the bottom of a heated, flat horizontal plate, heated on both sides. This uncertainty is also due to the fact that experimental results for turbulent free convection for that particular geometry are still very scarce, and additional data are needed. Because of relatively low convective heat transfer coefficient here, the effect of radiation correction becomes very important. Cases have been found in our experimentation where this correction for some specimens amounted to more than 50 % of the total heat transferred. Because of its emphasis on the radiation aspects in this case, and since both sides of plate were heated, the present investigation may be considered the first of its kind. The maximum total experimental error is calculated as ± 15 %.

A general comparison of the various experimental and analytical correlations is shown in Figs. 5 and 7, to stress the degree to which the results from the lit-

erature still differ from each other. It is also believed that, for the space environment, the present experiment shows that radiation cooling of electronics is more promising than free-convective cooling, where characteristic velocities are proportional to one half power of the Grashof number. With weak gravitational acceleration, Grashof numbers will be small, and effects of convective cooling negligible.

REFERENCES

1. Stewartson, K.: On Free Convection from a Horizontal Plate. ZAMP, vol.IXa, 1958, pp. 276-282.

2. Eckert, E. R. G., and Drake, R. M., Jr.: Heat and Mass Transfer. McGraw-Hill, 1959.

3. Bandrowski, J., and Rybski, W.: Analysis of Heat Transfer in Free Convection on Horizontal Plates. Chemical Engineering, vol. 3, 1975, pp. 3 - 16,(in Polish).

4. Eckert, E. R. G., and Jackson, T. W.: Analysis of Turbulent Free-Convection Boundary-Layer on a Flat Plate. NACA Report 1015, 1951.

5. McAdams, W. H.: Heat Transmission, 3rd ed. McGraw-Hill, 1954.

6. Schlichting, H.: Boundary-Layer Theory, 7th ed. McGraw-Hill, 1979.

7. Sibulkin, M.: Heat Transfer Near the Forward Stagnation Point of a Body of Revolution. J. of Aeronautical Sciences, vol. 19, 1952, pp. 570 - 571.

8. Hrycak, P.: Heat Transfer from Impinging Jets to a Flat Plate with Conical and Ring Protuberances. Int. J. Heat Mass Transfer, vol. 27, 1984, pp. 2145-2154.

9. Saunders, O., and Fishenden, M.: Some Measurements of Convection by an Optical Method. Engineering, May 1935, pp. 483-485.

10. Miaymoto, M., et al.: Free Convection Heat Transfer from Vertical and Horizontal Short Plates. Int. J. Heat Mass Transfer, vol. 28, 1985, pp. 1733-1745.

11. Sugawara, S., and Michioyshi, I.: Heat Transfer from a Horizontal Flat Plate by Natural Convection. Trans. Jap. Soc. Mech. Engrs., vol. 21, no. 109, 1955, pp. 651-657, (in Japanese).

12. Schulenberg, T.: Natural Convection Heat Transfer to Liquid Metals Below Downward-Facing Horizontal Surfaces. Int. J. Heat Mass Transfer, vol. 27, 1984, pp. 433-441.

13. Singh, S. M., Birkebak, R. C., and Drake, R. M., Jr.: Laminar Free Convection Heat Transfer from Downward-Facing Horizontal Surfaces of Finite Dimensions. Progress in Heat and Mass Transfer, vol. 2, 1969, pp. 87-98.

14. Lewandowski, W. M., and Kubski, P.: Effect of the Use of the Balance and the Gradient Methods... Natural Convection... Wärme und Stoffübertragung, vol. 18, 1984, pp. 247-256.

15. Yousef, W.W., Tarasuk, J.D., and McKean, W.J.: Free Convection Heat Transfer from Upward-Facing Isothermal Horizontal Surfaces. J. of Heat Transfer, vol. 104, 1982, pp. 493-500.

16. Fishenden, M., and Saunders, O. A.: An Introduction to Heat Transfer, Clarendon Press, 1952.

17. Bosworth, R. L. C.: Heat Transfer Phenomena. Wiley, 1952.

18. Al Arabi, M., and El-Riedy, M. K.: Natural Convection Heat Transfer from Isothermal Horizontal Plates ... Int. J. Heat Mass Transfer, vol. 19, 1976, pp. 1399-1404.

19. Hassan, K. E., and Mohamed, S. A.: Natural Convection from Isothermal Flat Surfaces. Ibid., vol. 13, 1970, pp. 1873-1886.

20. Fujii, T., and Imura, H.: Natural Convection from Plate with Arbitrary Inclination. Ibid., vol. 15, 1972, pp. 755-767.

21. Ishiguro, R., et al.: Heat Transfer .. Flow Instability ... Nat. Conv. .. Horizontal Surfaces. Proceedings, 6th Int. Heat Transfer Conf., vol. 2, Toronto, Canada, 1978, pp. 229-234.

22. Aihara, R., et al.: Free Convection along the Downward-Facing Surface of a Heated Horizontal Plate. Int. J. Heat Mass Transfer, vol. 15, 1972, pp. 2535-2549.

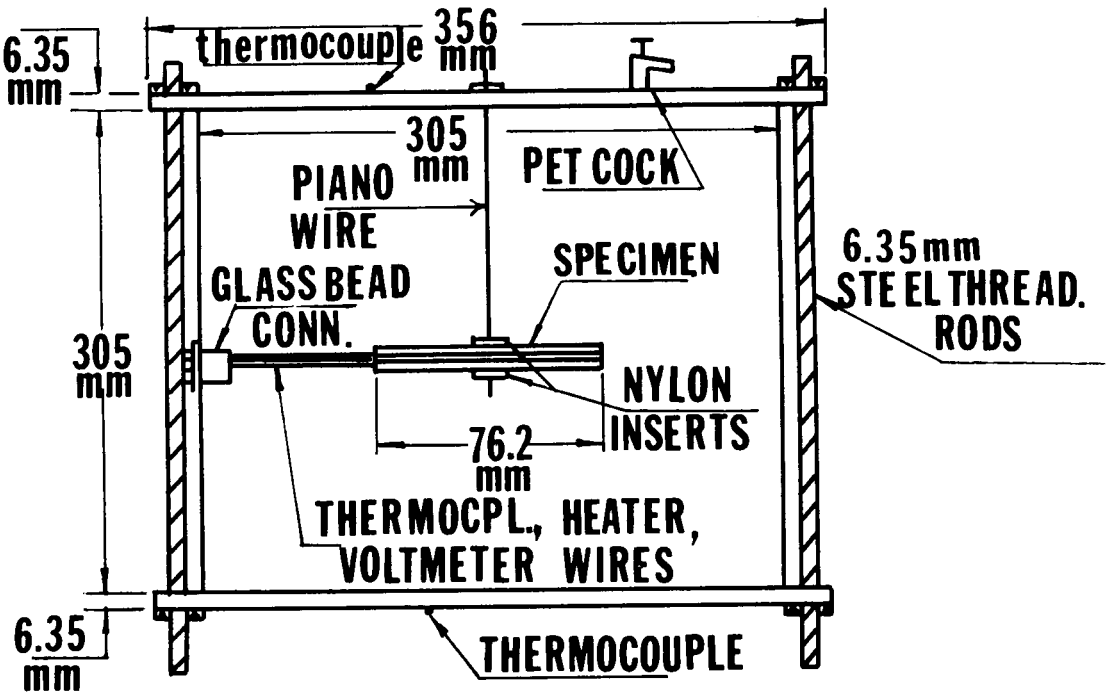

Figure 1. Experimental test set-up.

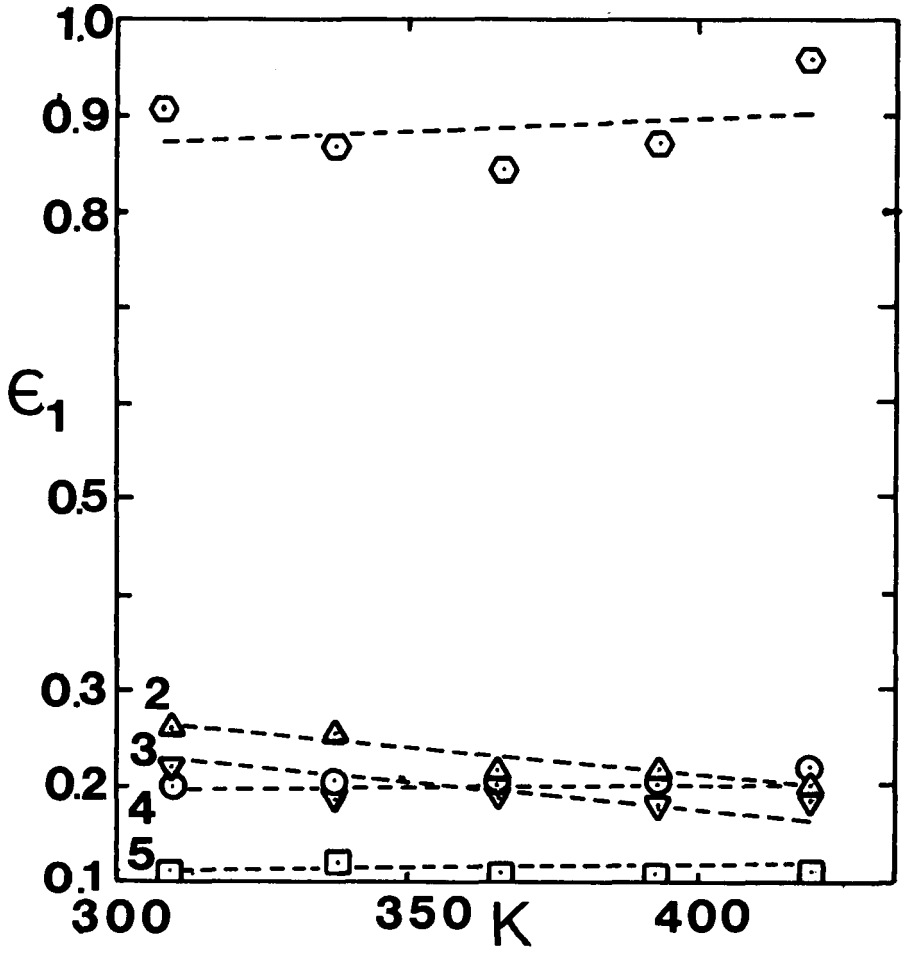

Figure 2. Emissivities of all samples tested. 1 - oxydized aluminum with Parson's black coating; 2 - oxydized aluminum with finger prints; 3 - oxydized aluminum, clean; 4 - oxydized aluminum, burnished; 5 - polished copper (all results by least squares fitting method; error margin: less than $\pm$ 6.5%).

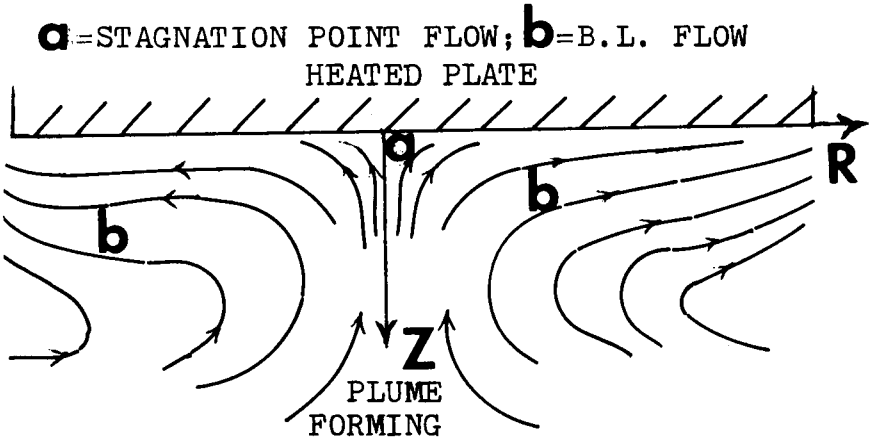

Figure 3. Schematic representation of natural convection near the center of a downward-facing, heated plate of finite dimensions.

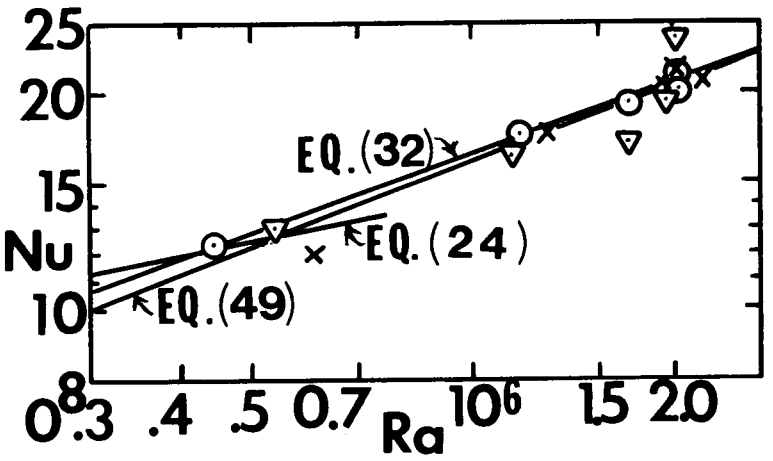

Figure 4. Average Nusselt number vs. Raleigh number for three specimens on horizontal, heated plate facing upward (maximum error ± 15%).

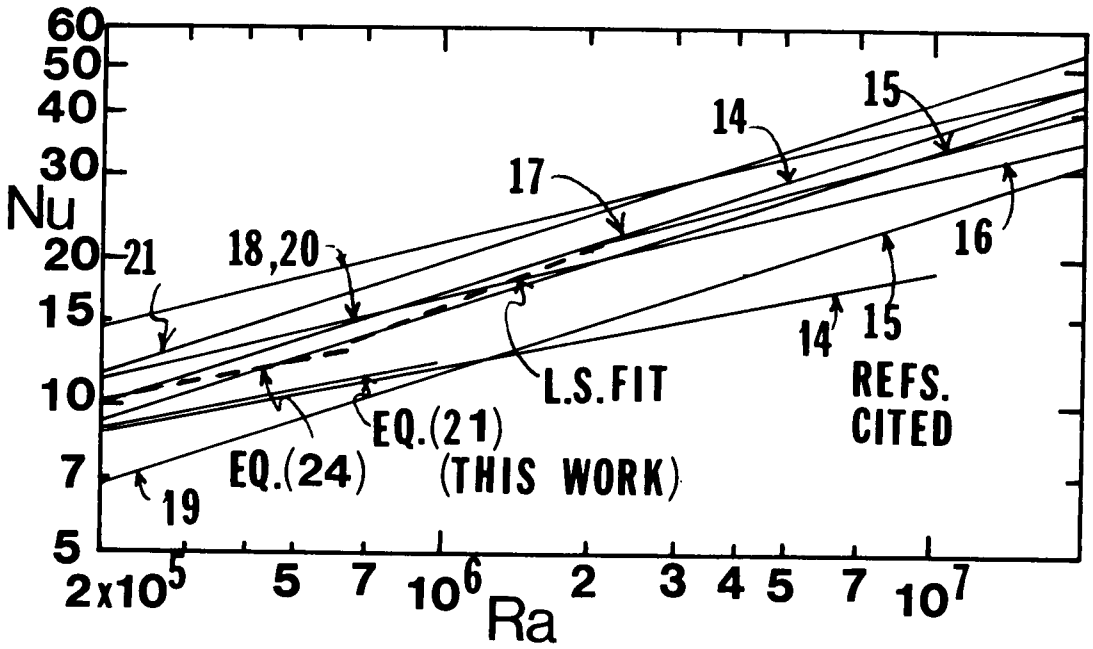

Figure 5. Comparison of results of various investigators, for a heated, upward-facing horizontal plate.

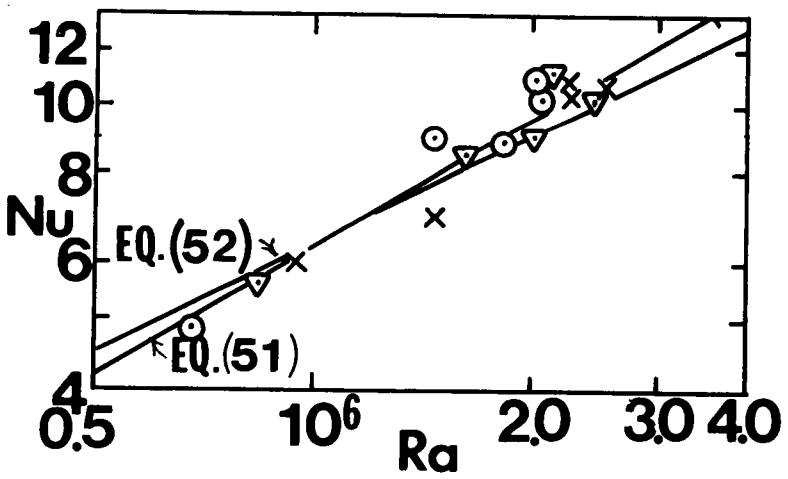

Figure 6. Average Nusselt number vs. Raleigh number for three specimens on horizontal, heated plate facing downward (maximum error: ± 15%).

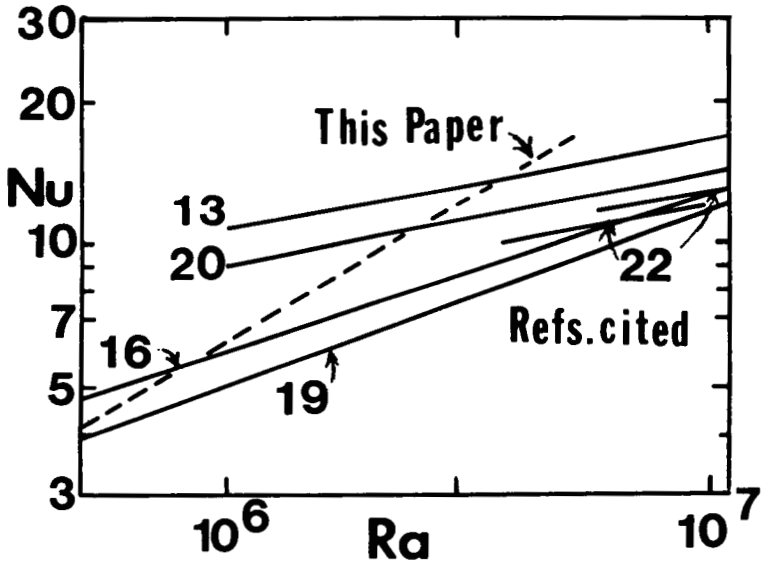

Figure 7. Comparison of results of several investigators, for a heated, downward-facing, horizontal plate.